

This is an electronic version of an article whose final and definitive form has been published in Ultramicroscopy (Volume 107, 2007, Pages 390395) (Elsevier); Ultramicroscopy is available online at: <http://www.sciencedirect.com/>.

AN ALGORITHM FOR REFINEMENT OF LATTICE PARAMETERS  
USING CBED PATTERNS

by A.Morawiec

Laboratoire d'Etude des Textures et Application aux Matériaux,  
Université Paul Verlaine – Metz,  
Ile du Saulcy, F-57045 Metz, France

Tel.: (+33)387315325, Fax:(+33)387315377, E-mail: nmmorawi@cyf-kr.edu.pl

**Abstract**

A new algorithm for calculation of lattice parameters from convergent beam electron diffraction (CBED) patterns has been developed. Like most of the previous approaches to the problem, it is an optimization procedure matching geometric elements of high order Laue zone (HOLZ) lines in experimental patterns to corresponding elements of kinematically simulated patterns. The procedure uses an original objective function based directly on the underlying algebraic equation of the HOLZ lines. Although the new approach requires crystal orientation parameters to be fitted alongside the strain components, it is easier to implement than methods used previously. It is also straightforward to apply to strain determination from multiple patterns. Numerical tests on dynamically simulated patterns show that in the case of one or two patterns, the new procedure gives results that are more reliable than the established method based on HOLZ line intersections. As an example application, the  $a$  and  $c$  parameters of a TiAl alloy are determined.

*PACS:* 61.14.x; 61.14.Lj; 81.40.Jj

*Keywords:* Convergent beam electron diffraction; Lattice parameters; Strain; Kossel microdiffraction; Titanium aluminide

## 1. Introduction

Lattice parameters are basic characteristics of crystalline materials. Deviations of the actual crystal lattice from a reference lattice can be determined from the geometry of high order Laue zone (HOLZ) lines present in convergent beam electron diffraction (CBED) patterns. The main application of this approach is the measurement of local elastic strains. The CBED based method offers reasonable accuracy of a few parts per ten thousand and a very good nanoscale spatial resolution (see, e.g., [1]). The resolution makes the CBED technique suitable for correlating strains with elements of microstructure. It is also a method of choice for investigation of strains in microelectronic devices. The main negative aspect of the CBED measurements is a stress relaxation caused by sample thinning.

The strategy of the CBED method is simple: the strain with respect to the reference lattice is calculated by matching strain dependent simulated patterns to experimental patterns. In principle, structural parameters can be obtained by fitting experimental and theoretical intensities [2, 3, 4] but that is difficult due to dynamic effects. Therefore, matching is based on simple geometric elements of HOLZ line patterns. In particular, following Zuo [5], distances between intersections of the HOLZ lines are fitted. Especially sensitive to line displacement are locations of small angle intersections, and they are considered to be the main source of information. However, locations of the small angle intersections are also very sensitive to errors in parameters of lines.

Another procedure is to match areas of triangles (or polygons) bounded by HOLZ lines [6]. This approach is based on the (questionable) assumption that the areas are less sensitive to dynamic effects at the intersections of HOLZ lines. The connection to the Zuo's method is simple because the triangle areas are directly related to the intersection distances via Heron's formula.

The matchings are usually implemented as optimization procedures with objective functions defined as sums of squared deviations between experimental and simulated distances or areas; e.g., [5, 6]. (For different approaches based on HOLZ line intersections see [7, 8].) Additional complications are due to the limited accuracy of the voltage and the camera length. The former is usually calibrated using a reference sample. As for the camera length, it is either fitted or eliminated by matching *ratios* of distances or areas.

This communication gives an account of a new procedure for computation of lattice parameters from the geometry of HOLZ line patterns. The method also uses optimization

but the objective function is different. It is based directly on the underlying algebraic equation of "K-lines" (in "K-line diffraction patterns" [9]) of which HOLZ lines in CBED patterns are a particular case. Therefore, the new approach is more fundamental than those used previously. For brevity, we will refer to it as a "K-Line equation based scheme" or KLEBS.

With a large camera length compared to a detector diameter, the conventional objective functions [5, 6] are negligibly influenced by small inaccuracies in a crystal orientation. This does not apply to KLEBS, in which correction to the orientation is fitted alongside strain and camera length. This is a major difference, because with increasing number of fitting parameters, the risk increases that the optimization will give false minima. Numerical tests prove otherwise; they show that KLEBS gives relatively reliable results.

Before proceeding to the main section, it must be mentioned that one CBED pattern is not sufficient for determination of all lattice parameters (or a complete strain tensor) [10] because the corresponding optimization problem is ill-conditioned [11]. One way to circumvent the ambiguity problem is to perform the calculation based on multiple patterns originating from one location. However, this causes additional experimental complications and a decrease in spatial resolution. Numerical tests indicate that KLEBS gives more reliable results than the established method based on line intersections when the number of patterns is small.

## 2. Procedure based on K-line equation

In matching experimental and simulated diffraction patterns, the latter are calculated numerous times. Since long computation times are needed for dynamic simulations, the matching must rely on kinematic calculations<sup>1</sup>. In the kinematic framework, the location of a HOLZ line is described by the (K-line) equation

$$2g \cdot k = g \cdot g , \tag{1}$$

where  $g$  is the reciprocal lattice vector corresponding to the line,  $k$  is the wavevector of the reflected beam satisfying  $k \cdot k = 1/\lambda^2$ , and  $\lambda$  denotes the radiation wavelength.

---

<sup>1</sup>Dynamic effects can be taken into account using additional measures. Frequently used is the "effective voltage approximation" [12, 13]. In some cases dynamic shifts of individual lines are calculated [14].

In brief, the main idea of KLEBS is to determine the lattice parameters which minimize  $\sum(2g \cdot k - g \cdot g)^2$ , where the sum is over reflections and wavevectors. This concept can be put into practice in a number of ways. In the particular implementation described here, the scalar products of eq.(1) are calculated in a Cartesian coordinate system linked to the crystal. The calculations require an initial approximation of the lattice parameters or, in the case of strain determination, a reference direct lattice. Let  $a_i^0$  be the  $i$ -th basis vector of the reference lattice in the Cartesian coordinate system linked to the crystal. In this system, the components of the reciprocal lattice vector  $g^0$  corresponding to the reflection  $(hkl)$  are

$$g^0 = (A^0)^{-1} [h, k, l]^T ,$$

where  $A_{ij}^0 = (a_j^0)_i$ , i.e.,  $A_{ij}^0$  is the  $i$ -th coordinate of the  $j$ -th basis vector. Let  $I$  be the identity matrix. A homogeneous displacement  $I + \varepsilon$  in the direct space alters the basis vectors  $a_i^0$  to  $a_i = (I + \varepsilon) a_i^0$ , whereas vectors of the reciprocal space are transformed to

$$g = (I + \varepsilon)^{-1} g^0 . \quad (2)$$

Knowing  $\varepsilon$ , one can directly calculate the actual basis vectors  $a_i$ , and hence, the standard lattice parameters  $a, b, c, \alpha, \beta, \gamma$ . Let  $L^0$  and  $\lambda^0$  be the initial assessments of the camera length and the wavelength, respectively. The symbols  $L$  and  $\lambda$  denote their unknown actual values. The corresponding parameters  $X^L$  and  $X^\lambda$  are defined by the expressions

$$L = L^0(1 + X^L) \quad \text{and} \quad \lambda = \lambda^0(1 + X^\lambda) ,$$

i.e. both  $X^L$  and  $X^\lambda$  are dimensionless and close to zero.

The wavevector is obtained from the HOLZ line location and the radiation wavelength via

$$k = \frac{1}{\lambda} \frac{v}{\sqrt{v \cdot v}} , \quad (3)$$

where  $v$  is a vector to a point on the diffraction line. The algebraic steps for getting  $v$  depend on the way the lines are described. Let the coordinate system linked to the microscope have the third axis along the optical axis of the system. If line parameters are the distance of the line from the pattern center  $\rho$ , and the directed angle between the outward-pointing normal to the line and the 1-axis  $\phi$ , then the vector (in the microscope system) to a point on the diffraction line can be expressed as

$$v^m = w + s w_p ,$$

where  $w = [\rho \cos \phi, \rho \sin \phi, -L]^T$  is a vector to the point closest to the pattern center,  $w_p = [-\sin \phi, \cos \phi, 0]^T$  is a vector perpendicular to  $w$  in the plane of the pattern, and  $s$  is a number parameterizing the line (Fig.1). The range of  $s$  must be small because, in fact, the HOLZ traces are conic sections, and only sufficiently short fragments can be approximated by straight lines. With the orientation of the crystal described by an orthogonal matrix  $R$ , the vector  $v$  in the Cartesian coordinate system linked to the crystal is given by

$$v = Rv^m .$$

The orientation is known only based on the approximate reference lattice parameters  $a_i^0$ ; let that orientation be given by an orthogonal matrix  $R^0$ . The actual orientation  $R$  is a product

$$R = R^0 R^X$$

where  $R^X$  is an orthogonal matrix corresponding to a small unknown orientation correction. The matrix  $R^X$  depends on three parameters. One can conveniently choose them to be the Rodrigues parameters  $X_i^R$  ( $i = 1, 2, 3$ ) so

$$R_{ij}^X = ((1 - X_k^R X_k^R) \delta_{ij} + 2X_i^R X_j^R - 2\epsilon_{ijk} X_k^R) / (1 + X_l^R X_l^R) ,$$

where  $\delta_{ij}$  is the Kronecker's delta,  $\epsilon_{ijk}$  is the permutation symbol, and summation convention is assumed; see, e.g. [15].

Based on the  $g$  vectors (2) for a number of reflections and  $k$  vectors (3) determined for some points on the corresponding HOLZ lines, one can define

$$\psi = \sum (2k \cdot g - g \cdot g)^2 , \quad (4)$$

where the sum is over the reflections and points used, and  $\psi$  depends on the unknown  $\varepsilon$ ,  $X_i^R$ ,  $X^L$  and  $X^\lambda$ :  $\psi = \psi(\varepsilon, X_i^R, X^L, X^\lambda)$ . The parameters for which the  $\psi$  function takes a minimal value are calculated numerically. Some of the parameters can be fixed if the corresponding quantities are known; in particular, if the wavelength is assumed to be known exactly,  $X^\lambda$  is set to zero.

If multiple patterns are used, one simply needs to add a sum over all patterns in eq.(4). This, however, has a significant influence on the number of fitted parameters. With the number of patterns being  $n$ , the optimization parameters are the sought-after components of  $\varepsilon$ ,  $3n$  orientation parameters  $X_i^R$ ,  $n$  camera length corrections  $X^L$  (and possibly one or  $n$  wavelength corrections  $X^\lambda$ ).

The above optimization problem is non-linear. The expression  $2k \cdot g - g \cdot g$  linearized with respect to small  $\varepsilon$ ,  $X_i^R$ ,  $X^L$  and  $X^\lambda$  takes the form

$$2k \cdot g - g \cdot g \approx 2g^0 \cdot \left( (R^0 R^X - \varepsilon R^0) k^0 + R^0 (X^L [0, 0, k_3^0]^T - \xi k^0) + \varepsilon g^0 - g^0/2 \right), \quad (5)$$

where the matrix  $R^X$  depends on the parameters  $X_i^R$  through  $R_{ij}^X = \delta_{ij} - 2\varepsilon_{ijk} X_k^R$ ,  $k^0$  is given by  $k^0 = v^0 / (\lambda^0 \sqrt{v^0 \cdot v^0})$ ,  $v^0 = w^0 + fw_p$ ,  $w^0 = [\rho \cos \phi, \rho \sin \phi, -L^0]^T$ , and  $\xi = X^L (k_3^0)^2 + X^\lambda$ . Inserting the above expression (5) into eq.(4) leads to a convex  $\psi$  function. The linearized version of the method was tested alongside its exact form.

Although we are focused here on CBED patterns, it is worth mentioning that KLEBS is also applicable to divergent beam X-ray diffraction (Kossel) patterns. The determination of lattice parameters by this classical technique was advanced in the sixties with the use of electron probe microanalyzers (see, e.g., [16, 17]), and is now being revived on a new level using scanning electron microscopy and digital cameras [18, 19]. The only modification of the described algorithm needed to get lattice parameters from Kossel patterns is a proper calculation of the  $v^m$  and  $v^0$  vectors.

### 3. Tests

Testing the reliability of a strain determination procedure is convincing if the output of the procedure can be compared to correct results. A simple approach is to simulate patterns with known lattice parameters, and then use these patterns to retrieve the parameters. Because of the presence of dynamic effects in CBED patterns, dynamic simulations are applicable. Our simulations were based on the Bloch wave scheme; see Fig.2. For simplicity, *Fig.2* absorption was neglected, and the Debye-Waller temperature factor was set to zero. The example test was based on five Si patterns corresponding to zone axes  $[1\ 3\ 0]$ ,  $[1\ 5\ 0]$ ,  $[2\ 3\ 0]$ ,  $[1\ 3\ 3]$  and  $[1\ 3\ \bar{3}]$ ; the patterns were simulated for very favorable conditions with visibility of high index reflections, large camera length of 1600mm, detector size of 25.4mm  $\times$  25.4mm and relatively low voltage of 100kV (Fig.3). The voltage was assumed to be known exactly, *Fig.3* i.e., the parameter  $X^\lambda$  was set to zero.

The simulated patterns corresponded to a "strained" lattice which differed from the

reference lattice ( $a_1^0 = [5.43, 0, 0]^T$ ,  $a_2^0 = [0, 5.43, 0]^T$ ,  $a_3^0 = [0, 0, 5.43]^T$  in Å) by the strain

$$\varepsilon = 10^{-4} \times \begin{bmatrix} 15 & 30 & 30 \\ & -30 & 30 \\ & & 15 \end{bmatrix}$$

given in the Cartesian crystal coordinate system.<sup>2</sup> Dynamic effects, the ambiguity, finite thickness of the HOLZ lines and their curvature lead to discrepancies between the true and recalculated strains. The deviation of the recalculated strain  $\varepsilon_r$  from  $\varepsilon$  was quantified by  $\Delta \equiv N(\varepsilon_r - \varepsilon)/N(\varepsilon)$ , where  $N$  is the Frobenius norm  $N(x) \equiv \sqrt{\text{Tr}(x^T x)}$ .

For instance, for the frequently used [1 3 0] pattern, the recalculated strain was

$$\varepsilon_r = 10^{-4} \times \begin{bmatrix} 13 & 28 & 30 \\ & -31 & 28 \\ & & 14 \end{bmatrix}, \quad \left( 10^{-4} \times \begin{bmatrix} 12 & 30 & 29 \\ & -35 & 27 \\ & & 13 \end{bmatrix} \right).$$

Here and below, the results of the linearized version are given in parentheses. The corresponding value of  $\Delta$  was 0.053 (0.100 for the linearized version), the fitted camera length was 1599.7 (1599.4), and the orientation correction  $R^X$  corresponded to a rotation by 0.29° (0.29°).

The values of  $\Delta$  for the remaining patterns [1 5 0], [2 3 0], [1 3 3] and [1 3  $\bar{3}$ ] were 0.286 (0.278), 0.172 (0.170), 0.777 (0.847) and 1.128 (1.333), respectively. The average value of  $\Delta$  for all five patterns is given in the first row of Table 1. Results of tests on multiple patterns are collected in the remaining rows. It is worth noting that there is not much difference between the method based on the exact form of eq.(1) and the one based on linear approximation of the equation. For comparison, data obtained conventionally by matching distances between HOLZ line intersections [20] are listed in the last two columns. The one marked by  $\mathcal{M}_{Fit}$  contains results for the camera length fitted as a parameter, the numbers in the column  $\mathcal{M}_{Ratio}$  were calculated based on distance ratios. The test indicates that KLEBS gives results more reliable than those of the conventional approach [5] if one or two patterns are used. With more than three patterns, the conventional approach is superior. The cause of degraded performance of KLEBS in the case of large  $n$  is the significantly

Table 1

---

<sup>2</sup>Regardless of the ambiguity, a complete strain tensor was recalculated even in the case of a single pattern. This allowed us to make the test simple. Different methods are compared based on the assumption that on average the magnitude of the bias caused by the ambiguity is similar for all considered methods.

increased number of fitted parameters. Limiting the number of free parameters improves the reliability of the results. For instance, conventional fitting of intersection distances for five patterns with exactly known camera lengths gives  $\Delta = 0.068$ , whereas for results obtained with KLEBS, the deviation is  $\Delta = 0.021$  (0.027). Although there is no simple way to get highly accurate camera lengths, the above is not just a speculative discussion because one may consider using an interactive iterative approach: apply consecutively conventional methods [5, 6] – to get the camera lengths, and KLEBS – to get a better evaluation of the strain tensor.

#### 4. Example application

As an example, the method was applied to the determination of  $a$  and  $c$  parameters of the tetragonal  $\gamma$  phase in the lamellar Ti-48(at.%)Al-2Cr-2Nb ( $\alpha_2 + \gamma$ ) alloy at room temperature. Four patterns collected with the camera length close to 461mm and fixed voltage of approximately 199.0kV were used; one of the patterns is shown in Fig.2a. The orientations were beyond low index zone axes (to alleviate the influence of dynamic effects) but they also gave a relatively large number of HOLZ lines in the patterns. Their zone axes were approximately [337 854 397], [600 044 799], [119 988 101] and [551  $\overline{357}$  755]. KLEBS applied to four patterns gives  $a = 4.0106\text{\AA}$ ,  $c = 4.0615\text{\AA}$  ( $a = 4.0106\text{\AA}$ ,  $c = 4.0614\text{\AA}$ ). The results of matching distances between line intersections with camera length fitted as a parameter ( $\mathcal{M}_{Fit}$ ) and those based on distance ratios ( $\mathcal{M}_{Ratio}$ ) are  $a = 4.0086\text{\AA}$ ,  $c = 4.0600\text{\AA}$  and  $a = 4.0086\text{\AA}$ ,  $c = 4.0599\text{\AA}$ , respectively.

*Fig.2*

Comparison of results for proper subsets (of the complete set of patterns) provides information about consistency of the analysis; a figure is put on the latter by assessing standard deviations of the data. The application of KLEBS, its linearized version,  $\mathcal{M}_{Fit}$  and  $\mathcal{M}_{Ratio}$  to all three- and two-pattern subsets (of the complete set of four patterns) gives on average  $a = 4.0106\text{\AA}$  and  $c = 4.0605\text{\AA}$  with the standard deviations of 0.0031 $\text{\AA}$  and 0.0028 $\text{\AA}$ , respectively.

From literature, the  $a$  and  $c$  parameters of  $\gamma$ -TiAl are found to be in the ranges 4.015 – 3.975 $\text{\AA}$ , 4.062 – 4.097 $\text{\AA}$ , respectively [21]. Thus, our results for  $a$  are within these limits close to the left bracket, while those for  $c$  are slightly beyond the lower bound.

## 5. Conclusions

Lattice parameters can be determined from CBED patterns using a procedure based directly on the kinematic (K-line) equation of HOLZ lines. The procedure is based on finding the parameters minimizing sums of squared deviations of experimentally determined left-hand sides of the equation from the exactly known right-hand sides. The main difficulty is that besides the lattice parameters and camera length, also the crystal orientation parameters must be fitted.

The approach was compared to the conventional matching of distances between line intersections. Both procedures are applicable to calculations utilizing multiple patterns. Numerical tests on simulated patterns indicate that the new method works better than the conventional methods if one or two patterns are used; with more than three patterns, conventional approaches give more reliable results.

In the presence of ambiguities, the reliability of results can be improved by combining a number of procedures. The simplest strategy is to use different approaches and verify whether they give similar results. In the case of discrepancies, consecutive application of a series of different methods and correction of the optimization conditions may ultimately lead to more reliable results.

## Acknowledgments

The author is grateful to Dr. Emmanuel Bouzy for the TiAl CBED patterns. The work was performed in the framework of a project supported by the European Community under a Marie Curie Intra-European Fellowship (contract no. MEIF-CT-2005-007762).

## References

- [1] A.Armigliato, R.Balboni, S.Frabboni, *Appl. Phys. Lett.* 86 (2005) 063508.
- [2] J.M.Zuo, J.C.H.Spence, *Ultramicroscopy* 35 (1991) 185.
- [3] C.Deininger, G.Necker, J.Mayer, *Ultramicroscopy* 54 (1994) 15.
- [4] Y.Ogata, K.Tsuda, Y.Akishige, M.Tanaka, *Acta Cryst. A* 60 (2004) 525.
- [5] J.M.Zuo, *Ultramicroscopy* 41 (1992) 211.
- [6] S.J.Rozeveld, J.M.Howe, S.Schmauder, *Acta Metall. Mater.* 40 (1992) S173.
- [7] T.Akaogi, K.Tsuda, M.Terauchi, M.Tanaka, *J. Electron Microsc.* 53 (2004) 11.
- [8] T.Yamazaki, T.Isaka, K.Kuramochi, I.Hashimotoa, K.Watanabe, *Acta Cryst. A* 62 (2006) 201.
- [9] J.M.Cowley, *Diffraction Physics*, Amsterdam, North-Holland, 1981.
- [10] H.J.Maier, R.R.Keller, H.Renner, H.Mughrabi, A.Preston, *Philos. Mag. A* 74 (1996) 23.
- [11] A.Morawiec, *Philos. Mag.* 85 (2005) 1611.
- [12] Y.P.Lin, D.M.Bird, R.Vincent, *Ultramicroscopy* 27 (1989) 233.
- [13] Y.Tomokiyo, S.Matsumura, T.Okuyama, T.Yasunaga, N.Kuwano, K.Oki, *Ultramicroscopy* 54 (1994) 276.
- [14] S.Krämer, J.Mayer, C.Witt, A.Weickenmeier, M.Rühle, *Ultramicroscopy* 81 (2000) 245.
- [15] A.Morawiec, *Orientations and Rotations: Computations in Crystallographic Textures*, Berlin, Springer, 2004.
- [16] D.L.Vieth, H.Yakowitz, *Rev. Sci. Instr.* 37 (1966) 206.
- [17] D.L.Vieth, H.Yakowitz, *Rev. Sci. Instr.* 39 (1968) 1929.
- [18] E.Langer, S.Däbritz, C.Schurig, W.Hauffe, *Appl. Surf. Sci.* 179 (2001) 45.

- [19] S.Berveiller, P.Dubos, K.Inal, A.Eberhardt, E.Patoor, *Mat. Sci. Forum* 490–491 (2005) 159.
- [20] A.Morawiec, in: W. Reimers (Ed.), *Residual Stresses VII, Proceedings of the 7th European Conference on Residual Stresses (Berlin)*, Trans Tech Publications Ltd, Switzerland, 2006, p.115.
- [21] R.V.Ramanujan, *Int. Mater. Rev.* 45 (2000) 217.

N° of patterns	KLEBS	$\mathcal{M}_{Fit}$	$\mathcal{M}_{Ratio}$
1	0.483 ( 0.546 )	0.971	1.614
2	0.259 ( 0.291 )	0.964	1.058
3	0.297 ( 0.283 )	0.200	0.225
4	0.326 ( 0.305 )	0.117	0.121
5	0.168 ( 0.209 )	0.070	0.070

**Table 1.**

A.Morawiec, *An algorithm for refinement of lattice parameters*

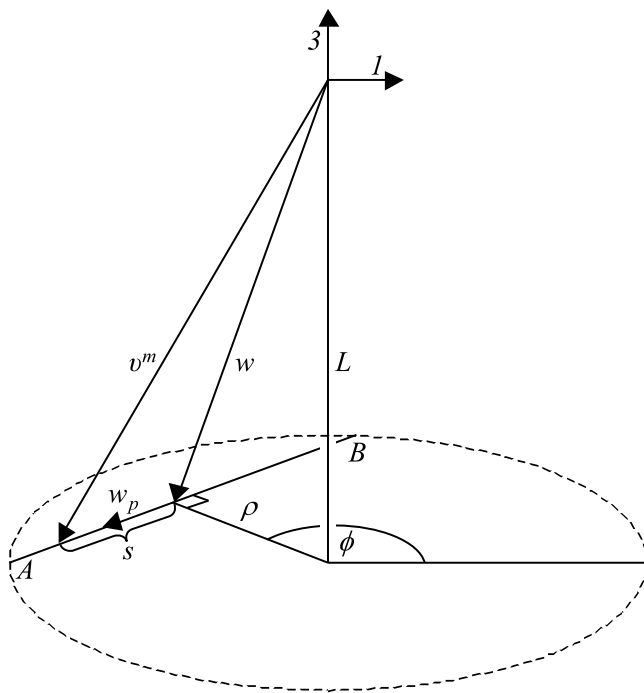


**Figure 1**

A.Morawiec, *An algorithm for refinement of lattice parameters*

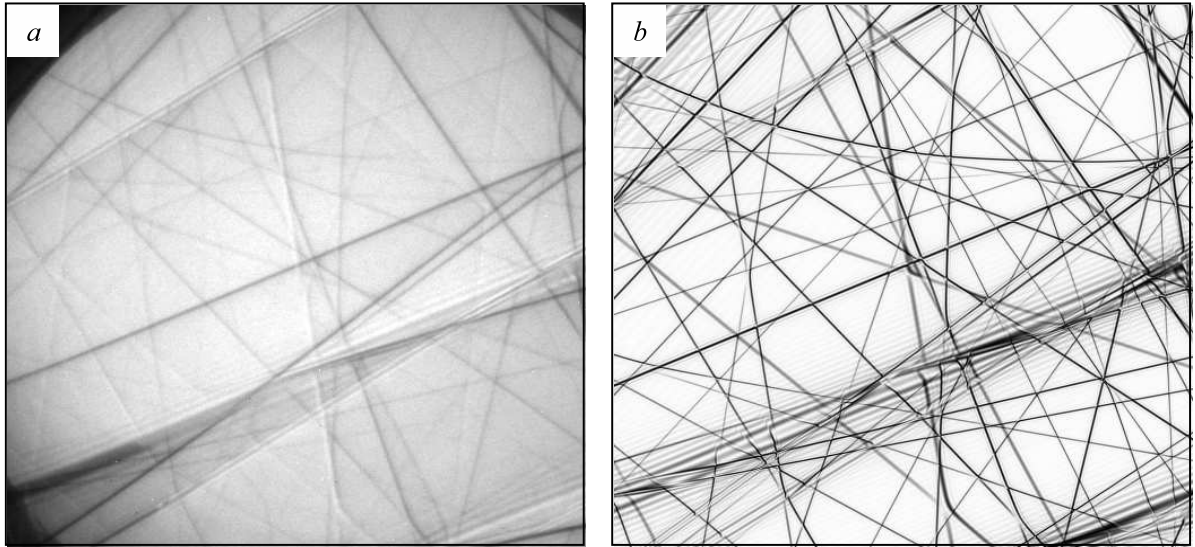


**Figure 2**

A.Morawiec, *An algorithm for refinement of lattice parameters*

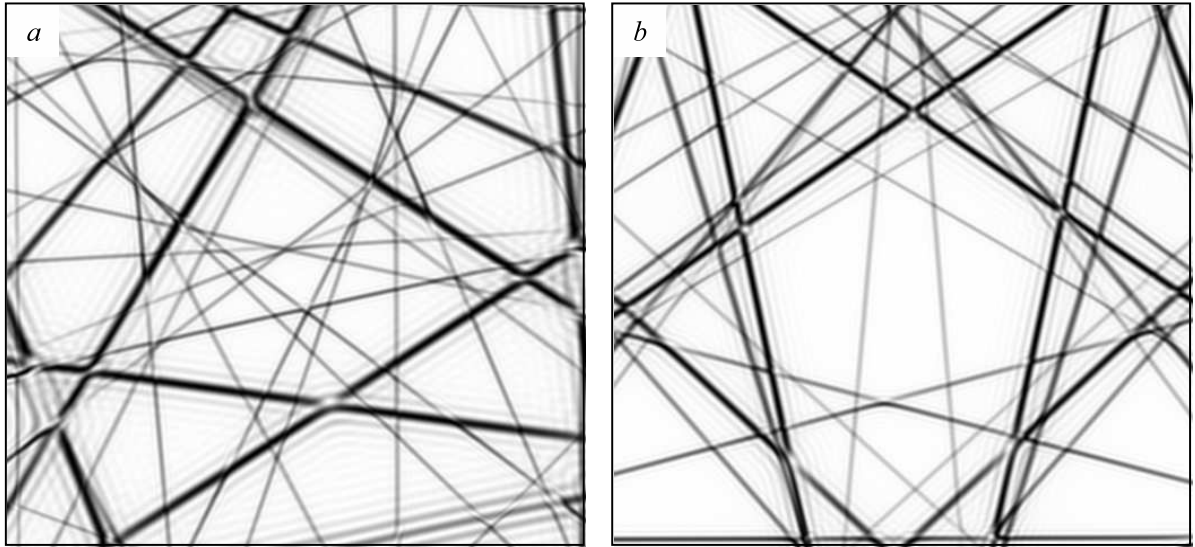


**Figure 3**

A.Morawiec, *An algorithm for refinement of lattice parameters*

## Captions

Table 1. The deviation ( $\Delta$ ) of recalculated strain from "true" strain. Each entry in rows 1–4 was obtained by averaging results from five different pattern combinations. Each entry of the last row (5) was obtained from a single set of five patterns. See text for more details.

Figure 1. Geometric characteristics of line  $AB$  (schematic).

Figure 2. An experimental (near  $[600\ 044\ 799] \approx [3\ 0\ 4]$ ) diffraction pattern of TiAl ( $a$ ) and corresponding dynamically simulated pattern ( $b$ ).

Figure 3. Two (out of five) simulated Si patterns used in the test:  $a$ )  $[1\ 3\ 3]$ ,  $b$ )  $[1\ 5\ 0]$ .